Chapter 1

Experiment

1.1 Discharge Apparatus

The design of the discharge apparatus was similar to the coaxial geometry used by Vasilyak and others [1]. This configuration has the benefit of minimizing the inductance of the system, which should aid in the propagation of the pulse through the system. Figure 1.1 is a to-scale illustration of the discharge apparatus.

The main portion of the discharge was provided by a borosilicate glass tube with Conflat flanges on either end. The glass portion of the tube had an inner diameter of 3.3 cm, an outer diameter of 4.0 cm, and a length of 22.9 cm. The total length of tube, including the glass tube, glass-to-metal transition, and flanges was 30 cm. The flanges served as the electrodes for the plasma. Seen here, the anode is located on the right, and the cathode/ground is located on the left.

The cathode was connected to a second glass tube with the same dimensions

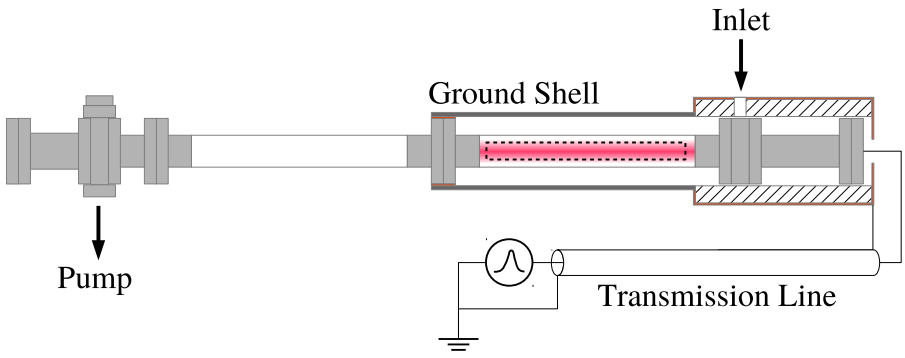

Figure 1.1: A scaled illustration of the discharge apparatus used in the RPND experiment.

as the first. This tube led to the pumping apparatus and served to electrically isolate it from the rest of the system. The cathode was also connected to ground through a cylindrical ground shell[1] which ran along the outside of the discharge tube. The ground shell was held in place against the cathode with a copper shim and Delrin shaft collar.

Two slots were milled into the ground shell on opposite sides. The slots were 3.8 cm by 30 cm and served to provide optical access to the discharge tube. The side of the ground shell opposite the cathode terminated at a copper sheet, 10 cm square. The copper sheet was perpendicular to the axis of the discharge tube and had a 5 cm hole for discharge tube to pass through. The ground shell was connected to the copper sheet with conductive copper tape.

The copper sheet was secured to a Teflon tube, approximately 20 cm in length

[1]While all of the outer conductors of the system are nominally at ground, it is believed that they would float to finite voltages with each pulse. This is a product of the nonideal impedance to ground and the high frequencies associated with the fast pulse.

with an inner diameter of about 7.5 cm and an outer diameter of 10 cm. The Teflon tube provided electrical isolation for the anode from structures supporting it. Surrounding the Teflon tube was a second ground shell composed of copper. This was connected to the first ground shell by a braided copper strap. The other end of the second ground shell ended in a similar square copper sheet, 10 cm on each side. This sheet was secured to the Teflon tube by nylon screws and seated against the ground shell for electrical contact.

The copper sheet also featured a HN bulkhead adapter for connection to the transmission line. The inner conductor of the bulkhead adapter was connected by a straight run of 5 cm of silicone-coated wire to a Conflat window angled at 45˚. The window was connected to a Conflat nipple, which in turn was connected to a double-sided flange used as the gas inlet (access was provided by a 2.54 cm diameter hole drilled into the surrounding Teflon tube). The other side of the double-sided flange was connected to the anode of the discharge tube.

The voltage pulse was provided by a FID pulser, supplied by ANVS, Inc. (model PT510NM). The amplitude of the pulse was fixed at 6.4 kV with a repetition rate of 1.0 kHz. Each pulse had a fixed width of 25 ns, with a 10%-90% rise time of approximately 4 ns and a roughly Gaussian shape. It is likely that the low conductivity of the gas preceding each pulse resulted in a doubling of the pulse potential as it reflected from the electrode. A SRS DG645 delay generator was used as the master clock in all experiments and was used to trigger the pulser. A 13.7 m transmission line was used in order to isolate reflections traveling back and forth between the pulser and anode. The cable used was RG213, and HN connectors

were used to prevent breakdown between the center conductor and ground.

The gas inlet connection was made through the double-sided flange via a 1/8" NPT hole. A 1/4" polyethylene tube was attached to the NPT connection via a NPT to 1/4" Swagelok adapater. The tube was then connected by Swagelok to a source of ultra-high purity (99.999%) helium. Throughout the experiment, the helium flow rate was fixed at 25.0 sccm with a digital flow controller, regardless of the operating pressure.

The discharge apparatus was pumped down by a oil-based roughing pump with an upstream zeolite trap. In each case, the system was evacuated by the roughing pump to the base pressure, approximately 15 mTorr, via a large-diameter tube. Based on this, the level of background impurities was estimated to be 80 ppm. This pump path was the closed off, and additional pumping was performed via two needle valve bypasses. The needle valves were used to adjust the pump rate in order to obtain the desired system pressure, monitored by two capacitance manometers with ranges of 10 and 100 Torr.

The assembled discharge apparatus can be seen in figure 1.2. The apparatus was supported on an optical breadboard 2.54 cm diameter posts and angle brackets. Attached to one of the angle brackets was a small optical breadboard with four bolts which served as physical references for aligning and positioning the apparatus.

All electrical measurements were made with a LeCroy 6100A WaveRunner oscilloscope which had a bandwidth of 1.0 GHz. Electrical connections to the oscilloscope were made with the shortest practical lengths of RG 50/U coaxial

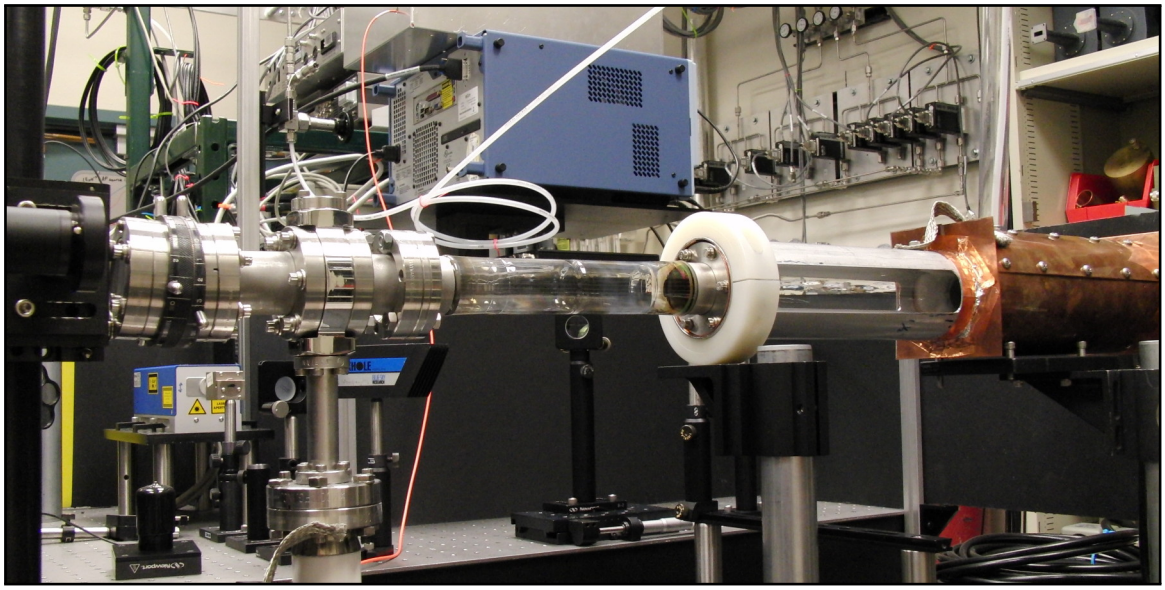

Figure 1.2: Photograph of the discharge apparatus.

cable and terminated at 50 Ω unless otherwise noted. The voltage of the pulser was monitored from an internal 1 : 1000 divider, and the current was via a current shunt located in a break of the outer conductor of the transmission line. The current shunt was composed of 9, low inductance, 1.0Ω resistors connected in parallel. Figure 1.3

Data were retrieved from the oscilloscope with a desktop computer via a GPIB connection. A LabView interface was used to interface with the oscilloscope and additional instruments. Analog inputs and outputs (such as laser control and pressure sensing) were handled by a SRS sr850 dsp lock-in amplifier which performed as an *ad hoc* data acquisition system.

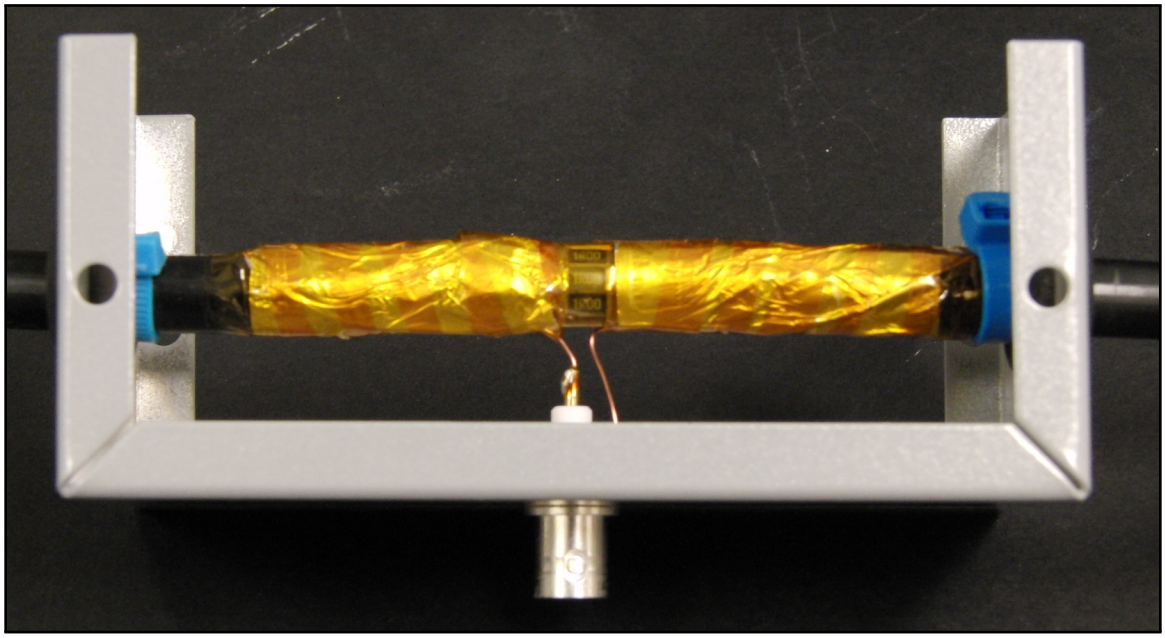

Figure 1.3: Photograph of the back-current shunt used to measure the current characteristics of the RPND.

1.2 Operating Procedure & Conditions

At the beginning of each day of operation, the system was first pumped down to base pressure. After this, the primary pump path was closed in favor of the needle valve bypasses. The helium flow was then initiated at 25.0 sccm. Then, the system pressure was adjusted to 3.0 Torr.

Once the pressure reached equilibrium, the pulser was turned on. The plasma was allowed to run at this condition for one hour in order to remove built up contamination on the walls and electrodes. During this time, the pressure of the system would typically drift downwards by several percent. Afterward, the pressure would be adjusted to the desired operating condition.

It was frequently necessary to turn off the pulser in between experiments. In these cases, once the pulser was turned on, the plasma was allowed to run for 15 minutes before any measurements were made. This was necessitated by observable changes in the emissions and current-voltage characteristics during the first 15 minutes of operation. Additional increases to this warm up time resulted in no appreciable changes to any of the measured data.

Measurements were made for a range of pressures, including: 0.3, 0.5, 1.0, 2.0 3.0, 4.0, 8.0, and 16.0 Torr. The lower limit was set by the pumping speed of the roughing pump. Difficulty in obtaining reliable plasma breakdown at pressures above 16.0 Torr set an upper limit on the pressure range. Experimental measurements of optical properties were obtained at three axial locations: 3.83, 11.45, and 19.07 cm relative to the boundary between the anode and the glass tube.

1.3 Initial Observations

Plasma characteristics could be divided into approximately three cases: low, intermediate, and high pressure. At the low pressures, 0.3, 0.5, and 1.0 Torr, it was difficult to initiate a discharge. Frequently, the plasma would have to be started at more moderate pressures, and then adjusted to the desired condition. At these conditions, the plasma was dim compared to the ambient room light and a dull purple. It appeared to be well separated from the walls. Visually, the diameter of the plasma was estimated to be about 2 cm, however this increased with pres-

sure. Also occurring at these conditions was a large amount of electronic noise. Nearby instruments, such as the computer mouse, and lock-in amplifier, would occasionally malfunction at these conditions.

At moderate pressures, 2.0, 3.0, and 4.0 Torr, the plasma expanded radially to fill the whole of the discharge volume. Compared to ambient conditions the plasma was bright with an orange-pink hue. Electrical interference disappeared at these conditions, and the plasma initiation was relatively easy. Nevertheless, at the beginning of each day several thousand pulses could be required before a visible plasma was formed. Interestingly, the plasma extended well past the cathode/ground and to the pumping section (connected to ground at a separate point). Presumably, this is a result of the relatively small cathode area compared to the large anode area. The build up of space charge limits the current extraction from the intended cathode, subsequently the electrode further downstream begins to contribute.

For the higher operating pressures, 8.0 and 16.0 Torr, the brightness of the plasma decreased, though not to the level of the low pressure discharge. In addition, the plasma remained volume-filling. However, it did not visibly extended past the cathode. Discharge initiation was difficult at these operating conditions and, as in the low pressure case, the plasma would have to be started at more amenable conditions. No electrical interference was noted for this pressure range.

Cursory examination of the voltage signal revealed a large number of reflections in the system. These can be seen in figure 1.4, a typical voltage waveform with overlaid arrows indicating the reflected pulses. These can be attributed to

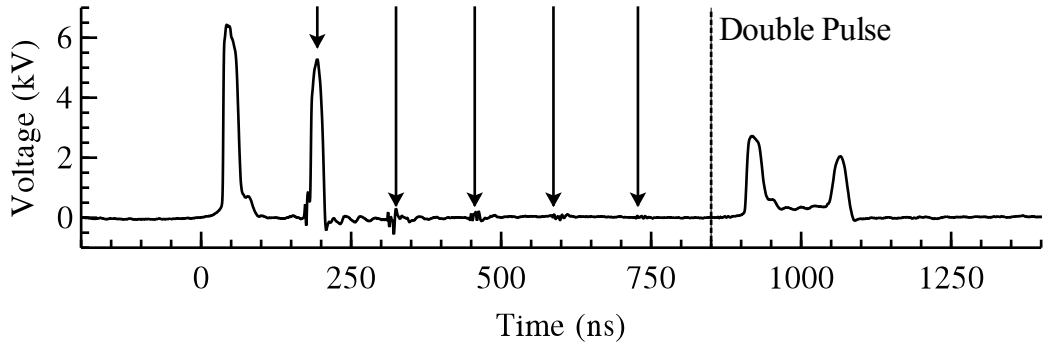

Figure 1.4: Typical voltage waveform of the RPND. Arrows indicate reflections back to the pulser. The pulser exhibited a double pulsing phenomena, indicated by the dotted line.

the impedance discontinuity at the electrode. Also observable in the waveform is a second pulse and its associated reflection. This is believed to be a peculiarity of the particular power supply used. The majority of the presented results, particularly those concerning the fast dynamics will only consider the initial pulse.

1.4 Field Calculations

The electric field characteristics of the discharge system was analyzed using a two-dimensional, electrostatic solver, Ansoft Maxwell 9. Figure 1.5 is a heat map on a logarithmic scale, of the electric field magnitude, with overlaid electric field vectors (in magenta). The electric field varies significantly over the length of the discharge apparatus, with a peak near the axial location of the glass tube followed by a monotonic decline. These characteristics are a large departure from simple case of two parallel electrodes in which the field is uniform throughout.

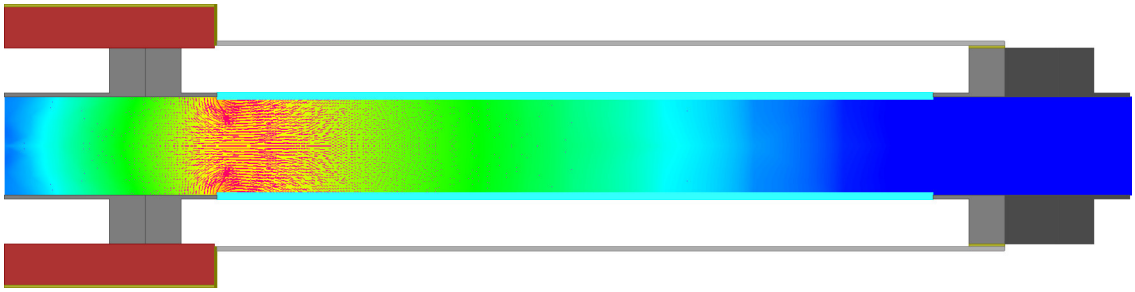

Figure 1.5: Heat map and vector plot of the electric field in the RPND discharge apparatus.

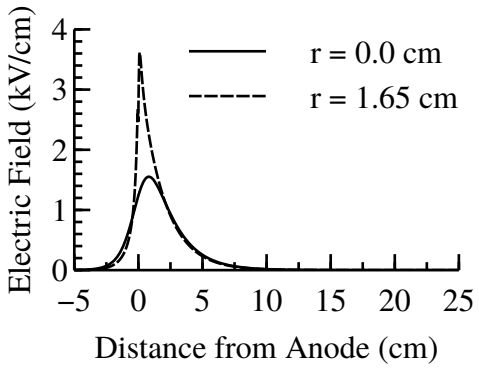

Figure 1.6: The magnitude of the electric field along the center and outside of the discharge apparatus.

This can be attributed to the presence of the external ground shield. Though this does complicate the field characteristics, the proximity of the ground results in a much higher electric field than would otherwise be achievable.

While the off-axis field lines all feature notable radial components, particularly close to the anode the center line does not. Figure 1.6 is a plot of the magnitude of the electric field along the central axis of the discharge apparatus and the outside, adjacent to the glass tube. The location of the anode is defined

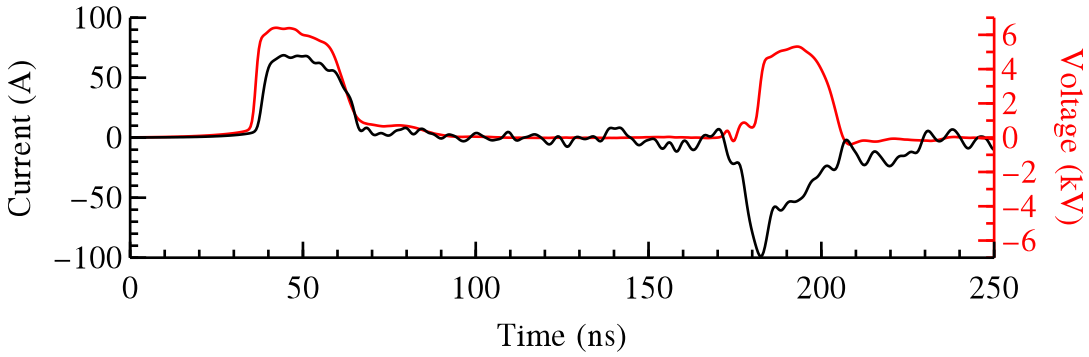

Figure 1.7: Higher resolution plot of the initial voltage and current pulse.

as the location of the glass-to-metal seal. The field close to the triple point at the seal is the highest at approximately 3.5 kV/cm, while the field along the axis peaks at about 1.5 kV/cm. At a distance of 2 cm from the anode, the electric field magnitude is roughly the same regardless of the radial coordinate. At the measurement locations of 3.83, 11.45, and 19.07 cm, the vacuum electric field was 4.8×10^5, 750, and 11 V/m respectively.

1.5 Energy Coupling

The energy coupling to the plasma for the first pulse was calculated by integration of the current and voltage product for the first incident and reflected pulse. Figure 1.7 is a closer view of the time domain under consideration at the 4.0 Torr condition. The voltage signal appears to be relatively unmarred by distortion or ringing. The current signal from the shunt does appear to involve a moderate degree of ringing. The ringing in the current signal increased at lower and higher

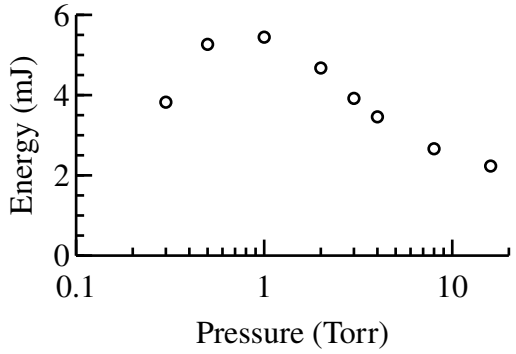

Figure 1.8: Plot of the energy coupled into the plasma with the first pulse as a function of pressure.

pressures and was most noticeable in the reflected pulse measurements.

Figure 1.8 shows the energy coupled to the plasma for the first incident pulse as a result of the above analysis. The coupled energy peaks at a pressure of 1.0 Torr and 5.5 mJ, before slowly decreasing. The uncertainty of these calculations is difficult to estimate as error may be introduced by the ringing of the current signal as well as timing differences between the current and voltage signals.

There are no literature values for the energy coupling of a helium RPND to compare to. However, several values exist for similar systems in other gases. Nishihara et al. recorded energy coupling which ranged from 1-2 mJ in 250 Torr of nitrogen [2]. Pancheshnyi et al., in the study of an air-propane mixture at 750 Torr, found that each pulse deposited about 1.9 mJ of energy. Laroussi and Lu's study of a atmospheric-pressure helium plasma jet estimated that the energy deposited per pulse was about 6-18 mJ based on the power consumption of the power supply [3]. Finally, Adamovich et al. used semi-analytic solution to one-

dimensional drift equations to estimate the per pulse energy density in 40 Torr of air as 0.02-0.07 mJ/cm^{-3} [4]. The energy density for the results in figure 1.8 ranged from about 0.01-0.02 mJ/cm^{-3}. Interestingly, Adamovich et al. observe that the majority of the energy deposition occurs in a very short time span after the initial breakdown of the gas. A similar model by Nikandrov et al. produced similar results [5].

Bibliography

[1] L M Vasilyak, S V Kostyuchenko, N N Kudryavtsev, and I V Filyugin. Fast ionisation waves under electrical breakdown conditions. *Physics-Uspekhi*, 37(3):247–268, March 1994.

[2] Munetake Nishihara, J. William Rich, Walter R Lempert, Igor V Adamovich, and Sivaram Gogineni. Low-temperature M=3 flow deceleration by Lorentz force. *Physics of Fluids*, 18(8):086101, 2006.

[3] M. Laroussi and X. Lu. Room-temperature atmospheric pressure plasma plume for biomedical applications. *Applied Physics Letters*, 87(11):113902, 2005.

[4] Igor V Adamovich, Munetake Nishihara, Inchul Choi, Mruthunjaya Uddi, and Walter R Lempert. Energy coupling to the plasma in repetitive nanosecond pulse discharges. *Physics of Plasmas*, 16(11):113505, 2009.

[5] Dmitry S. Nikandrov, Lev D. Tsendin, Vladimir I. Kolobov, and Robert R. Arslanbekov. Theory of Pulsed Breakdown of Dense Gases and Optimization

of the Voltage Waveform. *IEEE Transactions on Plasma Science*, 36(1):131–139, 2008.